ChemComm

RSC Publishing

COMMUNICATION

In situ visualization of Li-ion intercalation and formation of the solid electrolyte interphase on TiO_2 based paste electrodes using scanning electrochemical microscopy†

Cite this: *Chem. Commun.*, 2013, **49**, 9347

Received 19th June 2013,
Accepted 19th August 2013

DOI: 10.1039/c3cc44576c

www.rsc.org/chemcomm

Giorgia Zampardi,[ab] Edgar Ventosa,[a] Fabio La Mantia[b] and Wolfgang Schuhmann*[ab]

Scanning electrochemical microscopy (SECM) inside a glove box was used for the *in situ* visualization of solid electrolyte interphase (SEI) formation as well as Li-ion intercalation and de-intercalation on anatase TiO_2 based paste electrodes.

Li-ion intercalation and de-intercalation as well as the formation of the solid electrolyte interphase (SEI) are the most important phenomena in lithium ion batteries.[1] Formation and thickening of the SEI is one of the biggest sources of irreversible specific charge loss in active materials for negative electrodes. However, a stable SEI is indispensably necessary to use electrode materials with intercalation potentials located outside the stability window of the electrolyte. Information on SEI formation and its properties is obtained by post-mortem analysis of lithium ion batteries and *ex situ* techniques such as X-ray photoelectron spectroscopy (XPS)[2,3] and scanning electron microscopy (SEM).[4] *In situ* techniques for investigating the formation and nature of the SEI are highly important[1] and Fourier transform infrared spectroscopy (FTIR),[5] Raman spectroscopy,[6,7] and differential electrochemical mass spectrometry (DEMS)[8–10] were proposed.

Scanning electrochemical microscopy (SECM) operating in feedback mode can be used to detect surface and bulk electrochemical properties of a sample by analyzing its response to a local modification of the rate of the redox conversion of a free-diffusing redox species with an appropriately selected formal potential.[11] The SECM tip, typically a Pt disk electrode, locally oxidizes or reduces the redox species within the gap between the SECM tip and the sample surface. Depending on the rate of the back reaction at the sample the tip current is enhanced (positive feedback for reactive samples) or decreased (negative feedback for electrochemically inert samples). Importantly, feedback mode SECM specifically monitors modulations in the reaction rate of the redox mediator at the sample and is hence considered as a true chemical microscopy for determining interfacial properties. TiO_2 is currently attracting great interest as a negative electrode material for Li ion batteries.[12,13] The high operating potential of TiO_2 of *ca.* 1.7 V *vs.* Li/Li^+ decreases the specific energy of a related battery as compared to other negative electrode materials such as graphite. Concomitantly, it allows the negative electrode to operate within the stability window of the electrolyte. Thus, it was believed that either no SEI at all or only a very thin one is formed enabling the use of carbonaceous current collectors[14,15] and increasing safety and cyclability. The precise potential range at which a SEI is potentially formed on TiO_2 has been debated,[16–19] however, there is still no general agreement on this issue. In this communication, we show that the feedback mode of SECM can be successfully used to monitor the intercalation and de-intercalation of lithium into anatase TiO_2.

Intercalation of Li ions into a TiO_2 based paste electrode occurs at about 1.65 V *vs.* a Li/Li^+ reference electrode. Ferrocene (Fc), showing a redox potential of 3.22 V *vs.* Li/Li^+, was used as a free-diffusing redox species. Ferricinium cations (Fc^+) generated at the SECM tip at an applied potential of 3.5 V *vs.* Li/Li^+ reached the surface of the particles composing the TiO_2-based paste electrode. They are reduced back to Fc (Fig. 1a) with a reaction rate that enables a positive feedback and hence an increased tip current. Upon formation of the SEI on the surface of the TiO_2 particles, the reaction rate for the reduction of the Fc^+ decreases due to the insulating nature of the formed SEI (Fig. 1b).

Cyclic voltammetry at the SECM tip between 3.0 V and 3.6 V *vs.* Li/Li^+ with a scan rate of 10 mV s^{-1} was performed before and after SECM area scans to confirm the integrity of the SECM tip

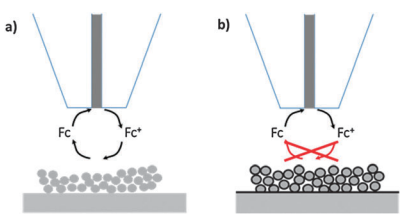

Fig. 1 Effect of the formation of the SEI on the feedback current at the SECM tip. The SEI modulates the reduction rate of Fc^+ at the paste electrode leading to a decreased feedback current.

[a] *Analytische Chemie – Elektroanalytik und Sensorik, Ruhr-Universität Bochum, Universitätstr. 150, D-44780 Bochum, Germany. E-mail: wolfgang.schuhmann@rub.de; Fax: +49 234 3214683*

[b] *Center for Electrochemical Sciences – CES, Ruhr-Universität Bochum, Universitätstr. 150, D-44780 Bochum, Germany*

† Electronic supplementary information (ESI) available. See DOI: 10.1039/c3cc44576c

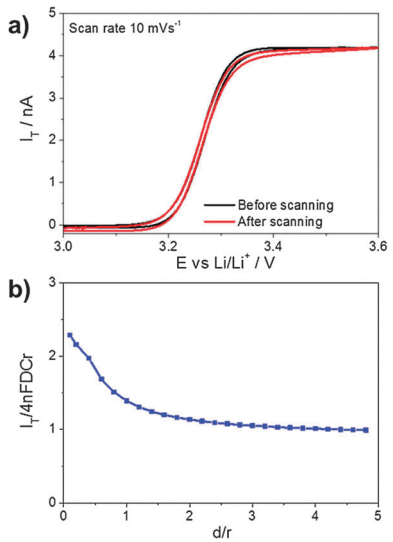

Fig. 2 (a) Cyclic voltammograms between 3.0 and 3.6 V *vs.* Li/Li$^+$ at a scan rate of 10 mV s^{-1} at the SECM tip positioned far away from the sample surface before and after the experiment. (b) Approach curve of the SECM tip towards the anatase TiO_2 paste electrode. *r* is the tip radius, *d* the distance of the SECM tip from the paste electrode. The electrolyte is PC : EC (1 : 1 by wt) containing 0.5 M $LiClO_4$ and 10 mM ferrocene.

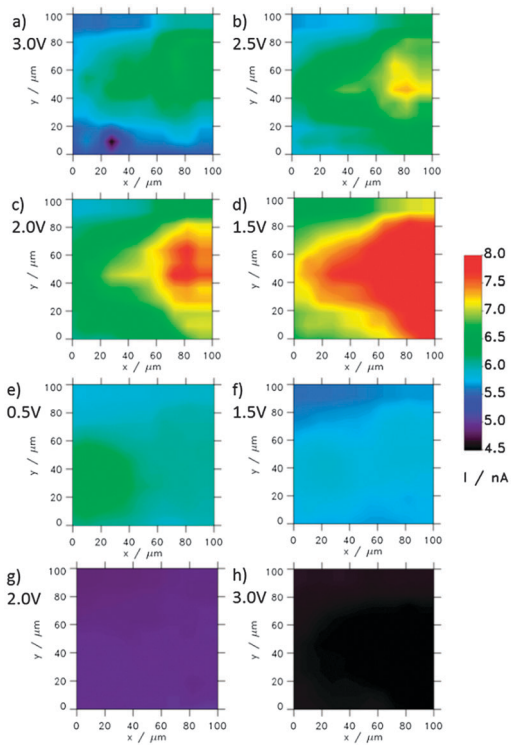

Fig. 3 Feedback-mode SECM images of the TiO_2 paste electrode in PC : EC (1 : 1 by wt) with 0.5 M $LiClO_4$ and 5 mM ferrocene at different sample potentials. From (a) to (e) the polarization potential is stepwise shifted cathodically from 3.0 V *vs.* Li/Li$^+$ to 0.5 V *vs.* Li/Li$^+$. From (e) to (h) the potential is shifted back anodically up to 3.0 V *vs.* Li/Li$^+$. All images are scaled to the same current color code.

during prolonged scanning in the feedback mode (Fig. 2a). Obviously, no contamination of the SECM tip occurs at a tip potential of 3.5 V *vs.* Li/Li$^+$ adjusted in the diffusion limited region of Fc oxidation. A typical SECM *z*-approach curve of the tip towards the TiO_2 paste electrode is shown in Fig. 2b and shows the positive feedback characteristic. Due to the fabrication procedure of the TiO_2 paste electrode by means of doctor blading, the electrode is porous with a thickness of about 25 to 30 μm and an average roughness of 3 to 5 μm. Although the paste electrode surface is supposed to mainly consist of the semiconducting TiO_2 particles, the added carbon black and the binder material may cover a considerable fraction of the surface. From the BET surface areas of the individual components and the relative composition, it is assumed that the surface contains about 55% TiO_2 particles.

Two kinds of experiments were performed starting from a freshly prepared TiO_2 paste electrode. First, after approaching the tip to the sample surface to a distance of about 7 μm, the local electrochemical activity of a 100 × 100 μm^2 area of the sample was visualized using feedback mode SECM (see Fig. 3). The sample potential was initially set to 3.0 V *vs.* Li/Li$^+$. After the SECM image was recorded, the sample potential was stepwise decreased by 0.5 V and after 30 min equilibration time again an SECM image was recorded. After recording the SECM image at the lowest sample potential of 0.5 V *vs.* Li/Li$^+$, the sample potential was stepwise increased to finally reach 3.0 V *vs.* Li/Li$^+$ again. Due to the fact that TiO_2 and carbon black particles are significantly smaller (below 1 μm) than the diameter of the SECM tip (10 μm), SECM images are averaged over a mixture of all components composing the paste electrode. Thus, the electrochemical properties of the paste electrode are supposed to appear homogenous in SECM images and local inhomogeneities represent variations in the tip-to-sample distance. At a starting potential of 3.0 V *vs.* Li/Li$^+$, the feedback current is positive at each grid point of the scanned area (Fig. 3a). By polarizing the TiO_2 paste electrode stepwise more cathodically (from Fig. 3b to d), the feedback current is increased due to the increasing driving force for the reduction of Fc$^+$. Especially by changing the sample potential from 2.0 V to 1.5 V *vs.* Li/Li$^+$ (Fig. 3c and d), a substantial increase of the feedback current is observed due to Li intercalation causing an increase in sample conductivity. Upon further decreasing the sample potential to 0.5 V *vs.* Li/Li$^+$ (Fig. 3e), the tip current suddenly drops, although it remains positive. Upon stepwise increasing the sample potential back to 3.0 V *vs.* Li/Li$^+$ (from Fig. 3f to h), the feedback current continuously decreases suggesting a further growth of the SEI concomitantly with the decreasing driving force of Fc$^+$ reduction. SECM images show an inverse local activity at a sample potential of 0.5 V *vs.* Li/Li$^+$ (Fig. 3e) as compared with the image at 1.5 V *vs.* Li/Li$^+$ (Fig. 3d) additionally supporting the influence of surface topography. The area on the right side of the image is obviously closer to the SECM tip as suggested by the higher positive feedback current as shown in Fig. 3a to d. Upon formation of the insulating SEI layer (Fig. 3e), the topography evidently leads to a less pronounced feedback current. At the Li-ion de-intercalation potential (at about 2.0 V *vs.* Li/Li$^+$; Fig. 3g), the current rapidly decreases. The inhomogeneity observed in Fig. 3 is due to changes of the tip-to-sample distance with the *x*,*y*-position, caused by the roughness of the porous electrode, which is in the same order of magnitude as the radius of the SECM tip. However, the topographic inhomogeneity in combination with the induced changes in the electrochemical properties of the porous electrode supports the interpretation that a completely blocking layer is formed as seen from the uniform drop of the feedback current upon SEI formation.

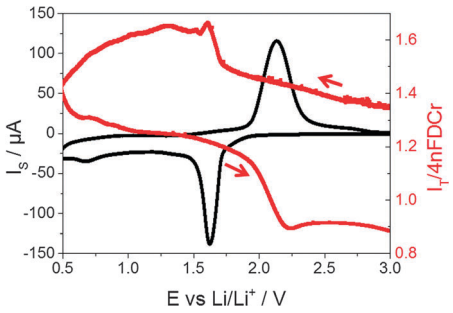

Fig. 4 Cyclic voltammogram at the anatase TiO_2 paste electrode at a scan rate of 0.1 mV s^{-1} (black line) and the corresponding feedback current at the SECM tip (red line). The electrolyte is PC : EC (1 : 1 by wt) containing 0.5 M $LiClO_4$ and 10 mM ferrocene.

Despite these experiments showing unequivocally the formation of a SEI on TiO_2 based paste electrodes, the onset potential of SEI formation could not be determined at a better accuracy than the potential difference sequentially applied to the sample.

In the second type of experiment, the tip was positioned at a distance of about 7 μm from the sample surface using a *z*-approach curve (see Fig. 4). To improve the time resolution, an experiment was performed in which the *x*,*y*-position of the SECM tip was kept constant after its approach to the predefined working distance. Again the tip was polarized to 3.5 V *vs.* Li/Li^+ for the diffusion-limited oxidation of Fc. Then, a cyclic voltammogram was recorded at the sample electrode with a scan rate of 0.1 mV s^{-1} in a potential range from 3.0 to 0.5 V *vs.* Li/Li^+ (Fig. 4).

The sample current, I_S, shows the peak for Li-ion intercalation at 1.65 V *vs.* Li/Li^+ and the de-intercalation process at 2.2 V *vs.* Li/Li^+ (Fig. 4, black line). At potentials below 0.8 V *vs.* Li/Li^+, an irreversible reduction peak is observed only in the first cycle which is indicative of SEI formation. Simultaneously, the feedback current, I_T, at the tip was recorded (Fig. 4, red line), which is initially increased due to the increasing driving force for Fc^+ reduction at the sample at more cathodic potentials. During intercalation of Li-ions into TiO_2, the feedback current at the tip increases rapidly which is indicative of an increased reaction rate for Fc^+ at the sample and hence an obviously increased conductivity of TiO_2 particles upon Li-ion intercalation. The feedback current continues to increase until a sample potential of 1.3 V *vs.* Li/Li^+. Starting from sample potentials as high as 1.3 V *vs.* Li/Li^+, the feedback current continuously decreases suggesting formation of a SEI already at substantially higher potentials than seen in the sample voltammogram (about 0.7 V *vs.* Li/Li^+).

Upon reversing the scan direction at a vertex potential of 0.5 V *vs.* Li/Li^+, the tip current continues to decrease until a sample potential of 1.9 V *vs.* Li/Li^+ is reached at which de-intercalation of Li-ions starts. This continuous decrease of the tip current suggests the growth of the SEI until Li-ion de-intercalation further decreases the reaction rate for Fc^+ leading to a drop in the normalized relative tip current from 1.2 to 0.9. The final normalized feedback current at the tip electrode is 0.46 lower than the normalized feedback current at the beginning of the measurement. At the end of the cyclic voltammogram at the paste electrode, the current at the tip exhibits a negative feedback which is typical for an insulating and/or inert material.

SECM feedback mode experiments demonstrate SEI formation starting at potentials as high as 1.3 V *vs.* Li/Li^+ on anatase TiO_2 nanoparticles. This is in contrast with earlier reports using Raman spectroscopy in which SEI formation was suggested to start above potentials of 2.0 V *vs.* Li/Li^+.[19] On carbon-based materials such as graphite, the SEI is formed at potentials of around 0.8 V *vs.* Li/Li^+ and the first products of electrolyte decomposition are observed at around 1.0 V *vs.* Li/Li^+ by means of DEMS.[8] It is not trivial to define the thermodynamic stability window for the used organic electrolytes; however, it should be close to the value obtained for graphite due to the chemical affinity between carbonaceous materials and organic electrolytes. From this point of view, the value obtained in this work for SEI formation on anatase TiO_2 seems more realistic.

The feedback mode of SECM was successfully applied for the *in situ* detection of SEI formation on porous electrodes used in Li-ion batteries. SECM feedback mode experiments demonstrate SEI formation starting at potentials as high as 1.3 V *vs.* Li/Li^+ on anatase TiO_2 nanoparticles. Moreover, a significant increase in the feedback current was observed upon intercalation of Li^+ in TiO_2. Future work will focus on the formation of SEI and its stability on carbonaceous materials taking into consideration that such processes are of utmost importance for the cycling life of Li-ion batteries.

Financial support by the DFG (SPP1473/WeNDeLIB, Schu929/11-1) is gratefully acknowledged. FLM is grateful for the financial support of the BMBF in the framework of the project "Energiespeicher" (03EK3005).

Notes and references

1 P. Verma, P. Maire and P. Novák, *Electrochim. Acta*, 2010, **55**, 6332–6341.
2 D. Aurbach, *J. Electrochem. Soc.*, 1996, **143**, 3809.
3 D. Aurbach, K. Gamolsky, B. Markovsky, Y. Gofer, M. Schmidt and U. Heider, *Electrochim. Acta*, 2002, **47**, 1423–1439.
4 L. J. Hardwick, H. Buqa, M. Holzapfel, W. Scheifele, F. Krumeich and P. Novák, *Electrochim. Acta*, 2007, **52**, 4884–4891.
5 M. Dollé, S. Grugeon, B. Beaudoin, L. Dupont and J.-M. Tarascon, *J. Power Sources*, 2001, **97–98**, 104–106.
6 J.-C. Panitz, F. Joho and P. Novak, *Appl. Spectrosc.*, 1999, **53**, 1188–1199.
7 F. Kong, R. Kostecki, G. Nadeau, X. Song, K. Zaghib, K. Kinoshita and F. McLarnon, *J. Power Sources*, 2001, **97–98**, 58–66.
8 F. La Mantia and P. Novák, *Electrochem. Solid-State Lett.*, 2008, **11**, A84.
9 F. La Mantia, F. Rosciano, N. Tran and P. Novák, *J. Electrochem. Soc.*, 2009, **156**, A823.
10 M. E. Spahr, T. Palladino, H. Wilhelm, A. Würsig, D. Goers, H. Buqa, M. Holzapfel and P. Novák, *J. Electrochem. Soc.*, 2004, **151**, A1383.
11 A. J. Bard, F. R. F. Fan, J. Kwak and O. Lev, *Anal. Chem.*, 1989, **61**, 132–138.
12 M. Wagemaker, W. J. H. Borghols and F. M. Mulder, *J. Am. Chem. Soc.*, 2007, **129**, 4323–4327.
13 Y. Ren, L. J. Hardwick and P. G. Bruce, *Angew. Chem., Int. Ed.*, 2010, **49**, 2570–2574.
14 X. Xin, X. Zhou, J. Wu, X. Yao and Z. Liu, *ACS Nano*, 2012, 11035.
15 H. B. Wu, X. W. D. Lou and H. H. Hng, *Chem.–Eur. J.*, 2012, **18**, 2094–2099.
16 R. Dominko, L. Dupont, M. Gaberšček, J. Jamnik and E. Baudrin, *J. Power Sources*, 2007, **174**, 1172–1176.
17 M. Wachtler, M. Wohlfahrt-Mehrens, S. Ströbele, J.-C. Panitz and U. Wietelmann, *J. Appl. Electrochem.*, 2006, **36**, 1199–1206.
18 R. Dedryvère, D. Foix, S. Franger, S. Patoux, L. Daniel and D. Gonbeau, *J. Phys. Chem. C*, 2010, **114**, 10999–11008.
19 S. Brutti, V. Gentili, H. Menard, B. Scrosati and P. G. Bruce, *Adv. Energy Mater.*, 2012, **2**, 322–327.